A new three-dimensional chaotic system and its modified generalized projective synchronization

Dai Hao(戴 浩), Jia Li-Xin(贾立新), Hui Meng(惠 萌), and Si Gang-Quan(司刚全)†

State Key Laboratory of Electrical Insulation and Power Equipment, School of Electrical Engineering, Xi'an Jiaotong University, Xi'an 710049, *China*

(Received 6 May 2010; revised manuscript received 27 August 2010)

Based on the Chen chaotic system, this paper constructs a new three-dimensional chaotic system with higher order nonlinear term and studies the basic dynamic behaviours of the system. The modified generalized projective synchronization has been observed in the coupled new three-dimensional chaotic system with unknown parameters. Furthermore, based on Lyapunov stability theory, it obtains the control laws and adaptive laws of parameters to make modified generalized projective synchronization of the coupled new three-dimensional chaotic systems. Numerical simulation results are presented to illustrate the effectiveness of this method.

Keywords: chaotic system, generalized projective synchronization, Lyapunov stability theory

PACS: 05.45.Ac, 05.45.Xt, 05.45.Pq **DOI:** 10.1088/1674-1056/20/4/040507

1. Introduction

Chaos is an ubiquitous and extremely complex nonlinear phenomenon. Since Lorenz found the first chaotic attractor (Lorenz chaotic attractor[1]) in the three-dimensional (3D) autonomous chaotic system in 1963, chaos has been intensively studied by many scholars in the last three decades.[2−4] Based on the Lorenz system, other chaotic systems were proposed in succession: Chen and Lü chaotic system[5] and Liu chaotic system,[6] etc. These chaotic systems have some simple nonlinear term and only have real equilibrium points. Furthermore Pecora and Carroll[7] first proposed a drive-response method to achieve synchronization between two chaotic systems since 1990 and then other methods have been proposed such as linear and nonlinear feedback control,[8] sliding mode control,[9] adaptive control[10,11] and liner matrix inequality (LMI) technique,[12] etc.

In this paper, based on the Chen chaotic system and by changing the nonlinear term of the Chen system, a new 3D chaotic system is constructed. This new 3D chaotic system has higher order nonlinear terms and 16 equilibrium points, 4 real equilibrium points and 12 complex equilibrium points. The basic dynamic behaviours of the system were studied and through the drive-response method to achieve the modified generalized projective synchronization in the coupled 3D chaotic system with unknown parameters. By improving the adaptive laws of parameters in Ref. [13] and selecting the appropriate Lyapunov function, we find that the synchronization errors converge faster and the effect of synchronization is better in comparison with the method in Ref. [13].

2. New 3D chaotic system

In Ref. [5], the Chen chaotic system is given by

$$\begin{cases} \dot{x} = a(y - x), \\ \dot{y} = (c - a)x - xz + cy, \\ \dot{z} = xy - bz, \end{cases} \tag{1}$$

where x, y, z are state variables and $a = 35$, $b = 3$ and $c = 28$ are parameters. Chen chaotic attractor and phase diagrams are shown in Figs. 1(a) and (b).

By changing the nonlinear term and the coefficients of some terms of Chen system and increasing the nonlinear terms in the first and second equation of state of the Chen system, a new 3D chaotic system is constructed. Higher order nonlinear term is the most important feature of the new 3D chaotic system, it can produce multiple equilibrium points. Equations of state are expressed as:

$$\begin{cases} \dot{x} = a(y - x) - yz, \\ \dot{y} = (x - z)^4 - 10xz + cy, \\ \dot{z} = x^2 + y^2 - bz. \end{cases} \tag{2}$$

†Corresponding author. E-mail: sigangquan@mail.xjtu.edu.cn

© 2011 Chinese Physical Society and IOP Publishing Ltd

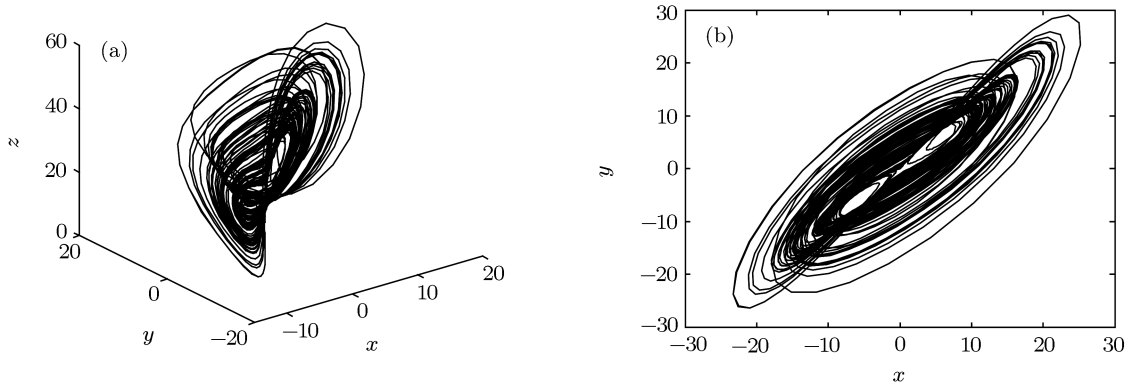


Fig. 1. Chaotic attractor for (a) Chen chaotic attractor (3D) and (b) the phase diagram (x–y).

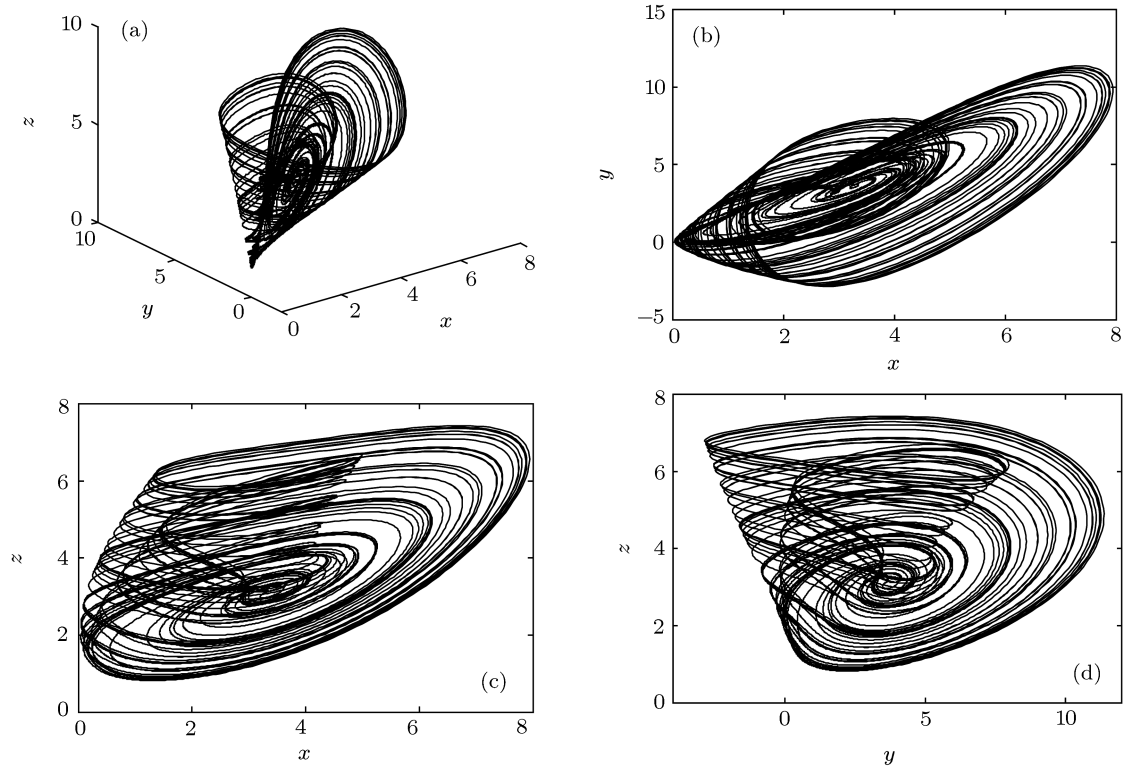


Fig. 2. The chaotic attractor of new chaotic system for (a) chaotic attractor in (x, y, z) space, (b) the phase diagram (x–y), (c) the phase diagram (x–z) and (d) the phase diagram (y–z).

The three Lyapunov exponents are respectively taken as

$$\lambda_1 = 2.8255, \quad \lambda_2 = 0, \quad \lambda_3 = -17.831.$$

Where x, y and z are state variables and

$$a = 35, \quad b = 8, \quad c = 28$$

are parameters. Chaotic attractors and phase diagrams of the new 3D chaotic system are shown in Figs. 2(a)–2(d); and bifurcation diagram of state variable x with the parameter c in Fig. 3. Only the local maximum and minimum of the state variable x are drawn in Fig. 3.

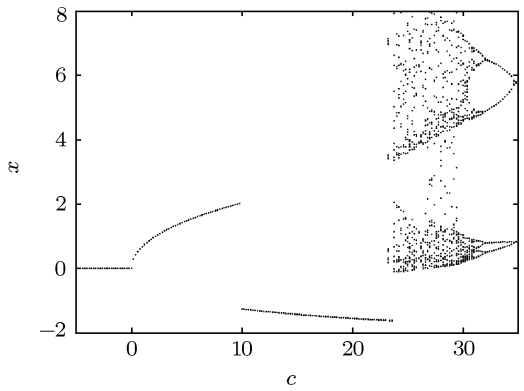


Fig. 3. Bifurcation diagram of state variable x with the parameter c.

3. Analysis of basic dynamic behaviours

3.1. Dissipation and attractor existence

The divergence of the system (2) is defined by

$$\boldsymbol{\nabla}\cdot\boldsymbol{V}=\frac{\partial\dot{x}}{\partial x}+\frac{\partial\dot{y}}{\partial y}+\frac{\partial\dot{z}}{\partial z}=-a+c-b=-15. \quad (3)$$

Because of $\boldsymbol{\nabla}\cdot\boldsymbol{V}<0$, the system (2) is a dissipative system and converges by the index rate of e^{-15t}.

Volume element V_0 shrinks to $V_0\mathrm{e}^{-15t}$ at the time of t. When $t\to\infty$, volume element shrinks to 0. Therefore, all trajectories of the system will be confined to a congregation, whose volume is 0. And the gradual movement behaviours are fixed in an attractor.

3.2. Equilibrium and stability

The equilibrium point of system (2) can be found by solving the following equations:

$$\begin{cases} a(y-x)-yz=0, \\ (x-z)^4-10xz+cy=0, \\ x^2+y^2-bz=0. \end{cases} \quad (4)$$

The obtained 16 equilibrium points (correct the result to keep four decimal digits) are given below:

$O(0,0,0), P_1(-1.7071,-1.7442,0.7446), P_2(3.3397,3.6607,3.0693), P_3(5.0819,6.8789,9.1431),$
$Q_1(27.8255+32.2695\mathrm{i},-33.0775+22.6764\mathrm{i},39.1052+36.9594\mathrm{i}),$
$Q_2(27.8255-32.2695\mathrm{i},-33.0775-22.6764\mathrm{i},39.1052-36.9594\mathrm{i}),$
$Q_3(31.8241+47.4640\mathrm{i},-48.3523+28.2915\mathrm{i},37.1852+35.6356\mathrm{i}),$
$Q_4(31.8241-47.4640\mathrm{i},-48.3523-28.2915\mathrm{i},37.1852-35.6356\mathrm{i}),$
$Q_5(48.6229+41.2237\mathrm{i},-40.9901+45.3397\mathrm{i},36.1616+36.4843\mathrm{i}),$
$Q_6(48.6229-41.2237\mathrm{i},-40.9901-45.3397\mathrm{i},36.1616-36.4843\mathrm{i}),$
$Q_7(40.5722+26.4940\mathrm{i},-25.5199+36.1135\mathrm{i},36.4070+38.3270\mathrm{i}),$
$Q_8(40.5722-26.4940\mathrm{i},-25.5199-36.1135\mathrm{i},36.4070-38.3270\mathrm{i}),$
$Q_9(4.2672+2.4346\mathrm{i},3.9561+3.2978\mathrm{i},2.1321+5.8588\mathrm{i}),$
$Q_{10}(4.2672-2.4346\mathrm{i},3.9561-3.2978\mathrm{i},2.1321-5.8588\mathrm{i}),$
$Q_{11}(-0.4692-2.5116\mathrm{i},-0.4142-2.4166\mathrm{i},-1.4696+0.5448\mathrm{i}),$
$Q_{12}(-0.4692+2.5116\mathrm{i},-0.4142+2.4166\mathrm{i},-1.4696-0.5448\mathrm{i}).$

This system has 4 real equilibrium points and 6 pairs of complex conjugate equilibrium points. In this paper, we only discuss the stability of the system (2) at 4 real equilibrium points.

The Jacobian matrix of the system (2) at the equilibrium point $O(0,0,0)$ is

$$J_0=\begin{bmatrix} -a & a & 0 \\ 0 & c & 0 \\ 0 & 0 & -b \end{bmatrix}. \quad (5)$$

Thus the corresponding characteristic equation can be obtained:

$$f(\lambda)=(\lambda+a)(\lambda-c)(\lambda+b)=0. \quad (6)$$

Three characteristic values can be obtained:

$$\lambda_1=-a,\quad \lambda_2=c,\quad \lambda_3=-b.$$

When $a=35$, $b=8$ and $c=28$, $\lambda_1=-35$, $\lambda_2=28$ and $\lambda_3=-8$. Here λ_2 is a positive real number, λ_1 and λ_3 are two negative real numbers. Therefore, the equilibrium point $O(0,0,0)$ is a saddle point. So, this equilibrium point $O(0,0,0)$ is unstable.

If we make the system (2) stable with respect to the equilibrium point $O(0,0,0)$, a, b, c must satisfy the following conditions:

$$a>0,\quad b>0,\quad c<0. \quad (7)$$

The Jacobian matrix of the system (2) at the equilibrium points $P_i(x_{i,0},y_{i,0},z_{i,0})$ $(i=1,2,3)$ is

$$J_i = \begin{bmatrix} -a & a - z_{i,0} & -y_{i,0} \\ 4(x_{i,0}-z_{i,0})^3-10z_{i,0} & c & -4(x_{i,0}-z_{i,0})^3-10x_{i,0} \\ 2x_{i,0} & 2y_{i,0} & -b \end{bmatrix} \tag{8}$$

with

$$A= 4(x_{i,0}-z_{i,0})^3+10x_{i,0}, \tag{9}$$

$$B= 4(x_{i,0}-z_{i,0})^3-10z_{i,0}, \tag{10}$$

$$J_i(\lambda) = \begin{bmatrix} \lambda + a & z_{i,0} - a & y_{i,0} \\ -B & \lambda - c & A \\ -2x_{i,0} & -2y_{i,0} & \lambda + b \end{bmatrix}. \tag{11}$$

For equilibrium point $P_1(-1.7071, -1.7442, 0.7446)$, substitute $a = 35$, $b = 8$, $c = 28$ and $x_{1,0} = -1.7071$, $y_{1,0} = -1.7442$, $z_{1,0} = 0.7446$ into Eqs. (9)–(11), then $A = -76.018$, $B = -66.393$ and characteristic roots can be obtained as

$$\lambda_1 = -16.905, \quad \lambda_2 = 0.9527 + 40.654\mathrm{i},$$
$$\lambda_3 = 0.9527 - 40.654\mathrm{i}.$$

Here λ_1 is a negative real number, λ_2 and λ_3 become a pair of complex conjugate eigenvalues with positive real parts. The equilibrium point $P_1(-1.7071, -1.7442, 0.7446)$ is a saddle-focus point, this equilibrium point is also unstable.

For equilibrium point $P_2(3.3397, 3.6607, 3.0693)$, substitute $a = 35$, $b = 8$, $c = 28$ and $x_{1,0} = 3.3397$, $y_{1,0} = 3.6607$, $z_{1,0} = 3.0693$ into Eqs. (9)–(11), then $A = 33.476$, $B = -30.614$ and characteristic roots can be obtained as

$$\lambda_1 = -24.907, \quad \lambda_2 = 4.9537 + 23.352\mathrm{i},$$
$$\lambda_3 = 4.9537 - 23.352\mathrm{i}.$$

Here λ_1 is a negative real number, λ_2 and λ_3 become a pair of complex conjugate eigenvalues with positive real parts. The equilibrium point $P_2(3.3397, 3.6607, 3.0693)$ is a saddle-focus point, this equilibrium point is also unstable.

For equilibrium point $P_3(5.0819, 6.8789, 9.1431)$, substitute $a = 35$, $b = 8$, $c = 28$ and $x_{1,0} = 5.0819$, $y_{1,0} = 6.8789$, $z_{1,0} = 9.1431$ into Eqs. (9)–(11), then $A = -217.11$, $B = -359.36$ and characteristic roots can be obtained as

$$\lambda_1 = 21.098, \quad \lambda_2 = -18.049+76.725\mathrm{i},$$
$$\lambda_3 = -18.049 - 76.725\mathrm{i}.$$

Here λ_1 is a positive real number, λ_2 and λ_3 become a pair of complex conjugate eigenvalues with negative real parts. The equilibrium point $P_3(5.0819, 6.8789, 9.1431)$ is a saddle point, this equilibrium point is also unstable.

3.3. Calculating the Lyapunov dimension

As is well known, the Lyapunov exponents measure the exponential rates of divergence or convergence of nearby trajectories in phase space, the largest value of positive Lyapunov exponents of this chaotic system is obtained as $\lambda_1 = 2.8255$. It is related to the expanding nature of different directions in phase space.

Another one Lyapunov exponent is $\lambda_2 = 0$. It is related to the critical nature between the expanding and the contracting nature of different directions in phase space.

The third Lyapunov exponent is $\lambda_3 = -17.831$. This is a negative Lyapunov exponent. It is related to the contracting nature of different directions in phase space.

The Lyapunov dimension of chaos attractors of this new chaotic system is fraction dimension, it is described as

$$\begin{aligned} D_L &= j + \frac{1}{|\lambda_{j+1}|}\sum_{i=1}^{j}\lambda_i \\ &= 2 + \frac{1}{|-17.831|}(2.8255 + 0) = 2.1585. \end{aligned} \tag{12}$$

3.4. The impact of system parameters

In this paper, choosing parameters $a = 35$, $b = 8$ and changing the value of c, we find that the system (2) shows different attractors and forms of movement.

(i) When $c = -5$, the system (2) is stable with respect to the equilibrium point $O(0, 0, 0)$ in Figs. 4(a) and 4(b).

(ii) When $c = 5$, the system (2) is stable with respect to the point $M_1(1.4809, 1.5049, 0.5573)$ in Figs. 5(a) and 5(b).

(iii) When $c = 9$, the system (2) is stable with respect to the point $M_2(1.9423, 1.9989, 0.9718)$ in Figs. 6(a) and 6(b).

(iv) When $c = 28$, the behaviours of the system (2) exhibit chaotic motion and result in the chaotic attractor in Figs. 7(a)and 7(b).

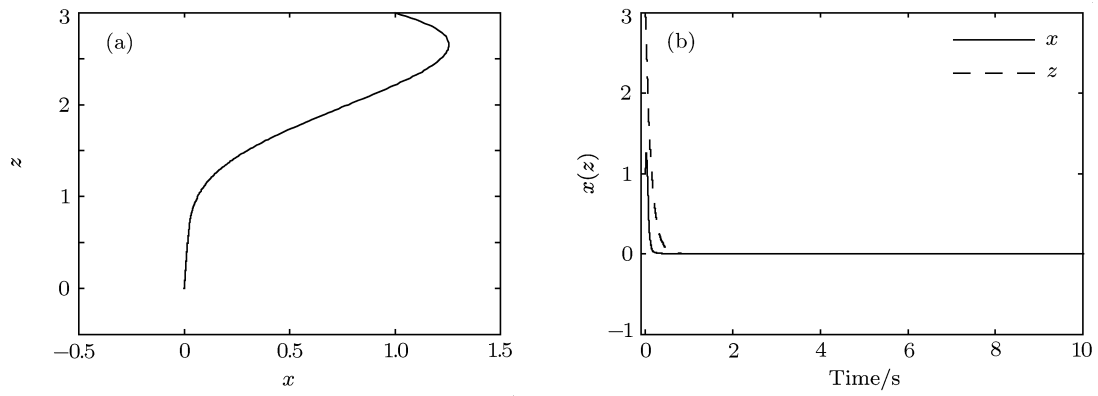


Fig. 4. The phase diagram and state trajectories for (a) phase diagram (x–z) and (b) state trajectories of x and z.

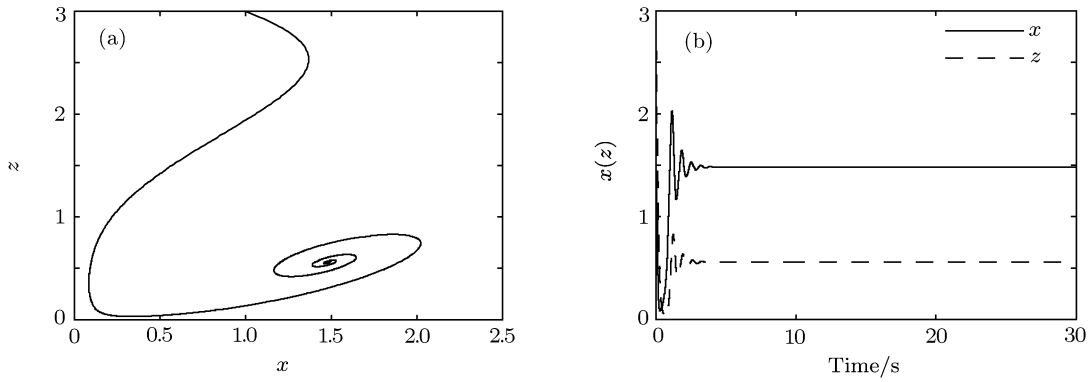


Fig. 5. The phase diagram and state trajectories for (a) phase diagram (x–z), (b) state trajectories of x and z.

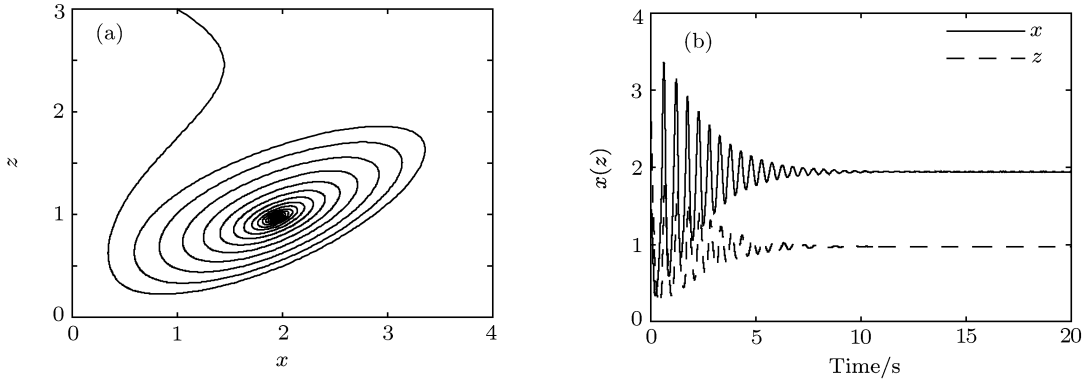


Fig. 6. The phase diagram and state trajectories for (a) phase diagram (x–z), (b) state trajectories of x and z.

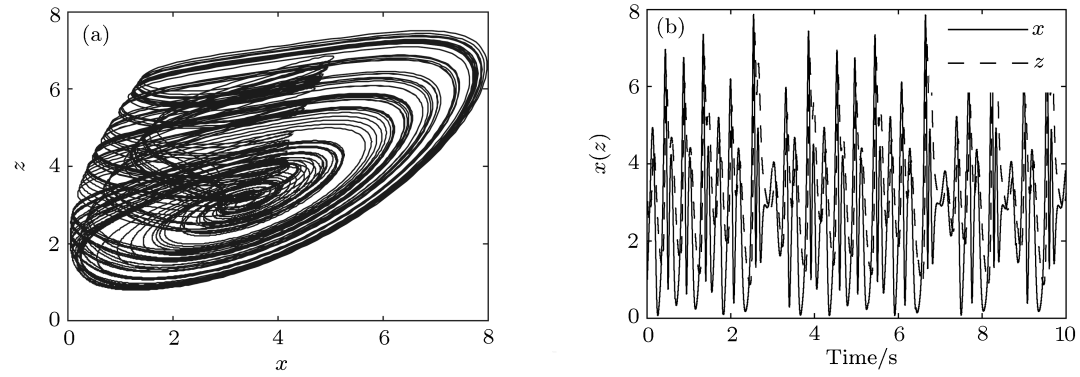


Fig. 7. The phase diagram and state trajectories for (a) phase diagram (x–z), (b) state trajectories of x and z.

(v) When $c = 31.5$, the behaviours of the system (2) exhibit quasi-periodic motion and result in the 2D torus as shown in Figs. 8(a) and 8(b).

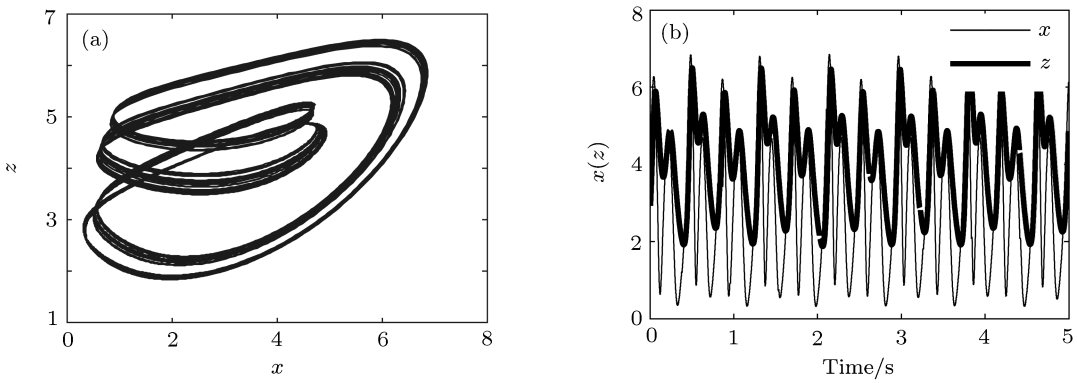


Fig. 8. The phase diagram and state trajectories for (a) phase diagram (x–z), (b) state trajectories of x and z.

(vi) When $c = 33$, the behaviours of the system (2) exhibit periodic motion and result in the limit cycle as shown in Figs. 9(a) and 9(b).

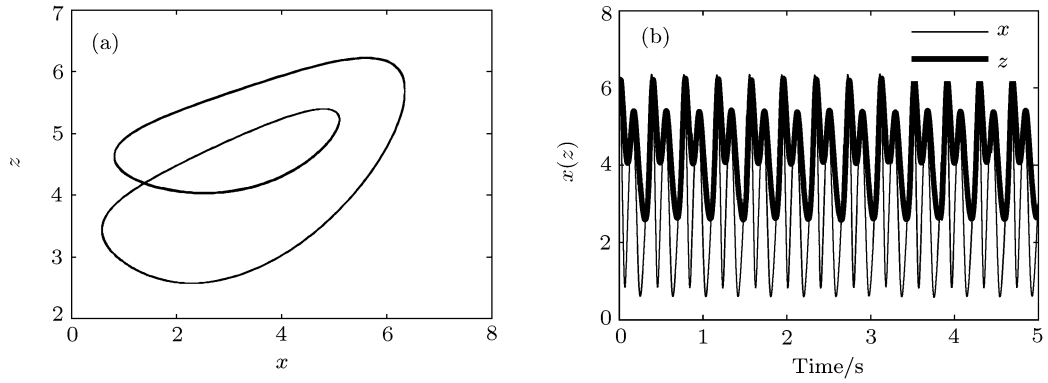


Fig. 9. The phase diagram and state trajectories for (a) phase diagram (x–z), (b) state trajectories of x and z.

(vii) When $c = 35$, the behaviours of the system (2) exhibit periodic motion and result in the simple limit cycle as shown in Figs. 10(a) and 10(b).

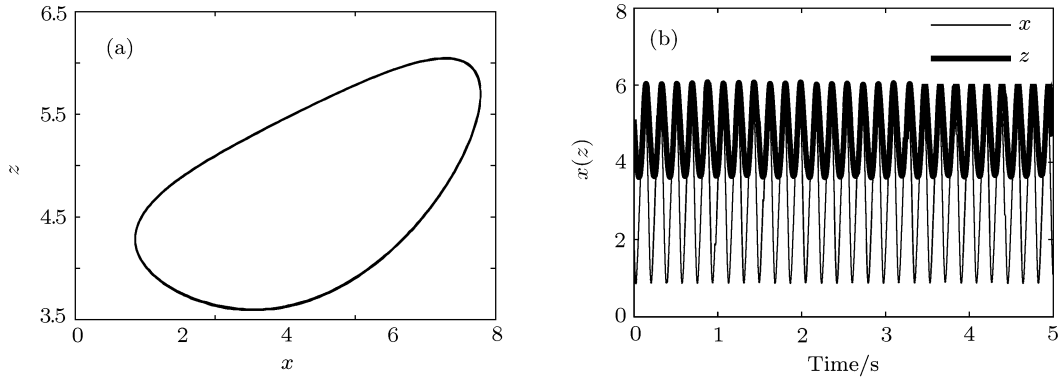


Fig. 10. The phase diagram and state trajectories for (a) phase diagram (x–z), (b) state trajectories of x and z.

4. Modified generalized projective synchronization in the coupled 3D chaotic system with unknown parameters

Consider the following nonlinear chaotic systems:

$$\dot{x} = F(x), \tag{13}$$

$$\dot{y} = F(y) + u, \tag{14}$$

where x, $y \in R^n$ are state variables; F is differentiable function of $R^n \to R^n$ and u is a controller.

The system (13) is a driving system and the system (14) is a response system. The following definition is modified generalized projective synchronization error:

$$e = y - Jx, \tag{15}$$

where

$$e = (e_1, e_2, e_3, \ldots, e_n)^{\mathrm{T}} \text{ and } J = \mathrm{diag}\{j_1, j_2, \ldots, j_n\}.$$

If there is a constant $j_i \neq 0$ $(i = 1, 2, \ldots, n)$, so that

$$\lim_{t\to\infty} e = \lim_{t\to\infty} [y(t) - Jx(t)] = 0, \tag{16}$$

where J is a matrix of scale factor.

Then we said that the system (13) and the system (14) achieve to generalized synchronization.

In this paper, we choose the following new 3D chaotic system as a driving system:

$$\begin{cases} \dot{x}_1 = a(x_2 - x_1) - x_2x_3, \\ \dot{x}_2 = (x_1 - x_3)^4 - 10x_1x_3 + cx_2, \\ \dot{x}_3 = x_1^2 + x_2^2 - bx_3. \end{cases} \tag{17}$$

The response system is:

$$\begin{cases} \dot{y}_1 = a_1(y_2 - y_1) - y_2y_3 + u_1, \\ \dot{y}_2 = (y_1 - y_3)^4 - 10y_1y_3 + c_1y_2 + u_2, \\ \dot{y}_3 = y_1^2 + y_2^2 - b_1y_3 + u_3, \end{cases} \tag{18}$$

where $x = (x_1, x_2, x_3)^{\mathrm{T}}$ and $y = (y_1, y_2, y_3)^{\mathrm{T}}$ are state variables; a, b, c and a_1, b_1, c_1 are unknown parameters of the driving system and the response system respectively; $u = (u_1, u_2, u_3)^{\mathrm{T}}$ is a controller.

Referring Ref. [13], we can write the driving system and the response system in the following form:

$$\begin{bmatrix} \dot{x}_1 \\ \dot{x}_2 \\ \dot{x}_3 \end{bmatrix} = \begin{bmatrix} -x_2x_3 \\ (x_1 - x_3)^4 - 10x_1x_3 \\ x_1^2 + x_2^2 \end{bmatrix} + \begin{bmatrix} x_2 - x_1 & 0 & 0 \\ 0 & 0 & x_2 \\ 0 & -x_3 & 0 \end{bmatrix} \begin{bmatrix} a \\ b \\ c \end{bmatrix}, \tag{19}$$

and

$$\begin{bmatrix} \dot{y}_1 \\ \dot{y}_2 \\ \dot{y}_3 \end{bmatrix} = \begin{bmatrix} -y_2y_3 \\ (y_1 - y_3)^4 - 10y_1y_3 \\ y_1^2 + y_2^2 \end{bmatrix} + \begin{bmatrix} y_2 - y_1 & 0 & 0 \\ 0 & 0 & y_2 \\ 0 & -y_3 & 0 \end{bmatrix} \begin{bmatrix} a_1 \\ b_1 \\ c_1 \end{bmatrix} + \begin{bmatrix} u_1 \\ u_2 \\ u_3 \end{bmatrix}. \tag{20}$$

With

$$g(x) = \begin{bmatrix} -x_2x_3 \\ (x_1 - x_3)^4 - 10x_1x_3 \\ x_1^2 + x_2^2 \end{bmatrix},$$

$$G(x) = \begin{bmatrix} x_2 - x_1 & 0 & 0 \\ 0 & 0 & x_2 \\ & 0 - x_3 & 0 \end{bmatrix}, \quad \Phi = \begin{bmatrix} a \\ b \\ c \end{bmatrix};$$

$$g(y) = \begin{bmatrix} -y_2y_3 \\ (y_1 - y_3)^4 - 10y_1y_3 \\ y_1^2 + y_2^2 \end{bmatrix},$$

$$G(y) = \begin{bmatrix} y_2 - y_1 & 0 & 0 \\ 0 & 0 & y_2 \\ 0 & -y_3 & 0 \end{bmatrix},$$

$$\Phi_1 = \begin{bmatrix} a_1 \\ b_1 \\ c_1 \end{bmatrix} \quad \text{and} \quad u = \begin{bmatrix} u_1 \\ u_2 \\ u_3 \end{bmatrix}.$$

The error system between the driving system (19) and the response system (20) can be expressed as

$$\begin{aligned} \dot{e} &= \dot{y} - J\dot{x} \\ &= g(y) + G(y)\Phi_1 - Jg(x) - JG(x)\Phi + u. \end{aligned} \tag{21}$$

The problem of generalized synchronization of the original system transforms into the stability of the error system.

In this paper, we choose the controller in the following form:

$$\begin{aligned} u = {} & -g(y) + Jg(x) - G(y)\Phi \\ & + JG(x)\Phi - N(f(t))e, \end{aligned} \tag{22}$$

where N is a constant and $N > 0$, $f(t) = |\sin(10t)| + 1$ and $f(t) \geq 1$.

Then $f'(t)$ can be defined in the following form:

$$f'(t) = \begin{cases} 10\cos(10t), & \sin(10t) > 0, \\ -10\cos(10t), & \sin(10t) < 0, \\ 10, & \sin(10t) = 0^+, \\ -10, & \sin(10t) = 0^-, \end{cases} \tag{23}$$

where $f'(t) \in [-10, 10]$.

Now, by substituting $g(x)$, $G(x)$, $g(y)$, $G(y)$ and Φ into Eq. (22), we can express the control laws as follows:

$$\begin{cases} u_1 = y_2y_3 - j_1x_2x_3 - a(y_2 - j_1x_2 - e_1) - Nf(t)e_1, \\ u_2 = -(y_1 - y_3)^4 + j_2(x_1 - x_3)^4 + 10[y_1y_3 - j_2x_1x_3] - ce_2 - Nf(t)e_2, \\ u_3 = -(y_1^2 + y_2^2) + j_3(x_1^2 + x_2^2) + be_3 - Nf(t)e_3. \end{cases} \tag{24}$$

Choose the adaptive law of unknown parameters Φ_1 in the following form:

$$\dot{\Phi}_1 = -Nf(t)[G(y)]^{\mathrm{T}}e, \tag{25}$$

where N is a constant and $N > 0$, N controls the speed of convergence of parameters Φ_1.

For the error system (21), we choose the Lyapunov function as

$$V = \frac{Nf(t)}{2}e^{\mathrm{T}}e + \frac{1}{2}\Psi^{\mathrm{T}}\Psi > 0, \tag{26}$$

where $\Psi = \Phi_1 - \Phi$ and $\dot{\Psi} = \dot{\Phi}_1$.

Substituting control law (22) into Eq. (21), we can express the error system by the following formula:

$$\dot{e} = G(y)\Psi - Nf(t)e. \tag{27}$$

In this paper, substituting $G(y)$ and Ψ into Eq. (27), we can express the error system by the following formula:

$$\begin{cases} \dot{e}_1 = (a_1 - a)(y_2 - y_1) - Nf(t)e_1, \\ \dot{e}_2 = (c_1 - c)y_2 - Nf(t)e_2, \\ \dot{e}_3 = -(b_1 - b)y_3 - Nf(t)e_3. \end{cases} \tag{28}$$

Then, taking the derivation of Eq. (26) with respect to time, we obtain

$$\begin{aligned} \dot{V} =& \frac{Nf'(t)}{2}e^{\mathrm{T}}e \\ &+ \frac{Nf(t)}{2}(\dot{e}^{\mathrm{T}}e + e^{\mathrm{T}}\dot{e}) + \frac{1}{2}(\dot{\Psi}^{\mathrm{T}}\Psi + \Psi^{\mathrm{T}}\dot{\Psi}) \\ =& \frac{Nf'(t)}{2}e^{\mathrm{T}}e + \frac{Nf(t)}{2}[(\Psi^{\mathrm{T}}[G(y)]^{\mathrm{T}} \\ &- Nf(t)e^{\mathrm{T}})e + e^{\mathrm{T}}(G(y)\Psi - Nf(t)e)] \\ &+ \frac{1}{2}[-Nf(t)e^{\mathrm{T}}G(y)\Psi + \Psi^{\mathrm{T}}(-Nf(t)[G(y)]^{\mathrm{T}}e)] \\ =& \frac{Nf'(t)}{2}e^{\mathrm{T}}e - N^2f(t)^2e^{\mathrm{T}}e \\ \leq& N(5 - N)e^{\mathrm{T}}e. \end{aligned} \tag{29}$$

If $N > 5$, then $V'(t) < 0$ and then $\lim_{t\to\infty} e(t) = 0$. Finally the generalized synchronization will be accomplished.

5. Simulation results

In what follows, by calculating system error e, we find that numerical simulation results can illustrate the effectiveness of this method to accomplish modified generalized projective synchronization in the coupled new 3D chaotic system with unknown parameters.

In this section, synchronization between the driving system (19) and response system (20) is demonstrated. The value of initial conditions of the driving system and the response system are

$$(x_1(0), x_2(0), x_3(0)) = (1, 2, 3),$$
$$(y_1(0), y_2(0), y_3(0)) = (10, 10, 10).$$

Choose unknown parameters of the driving system

$$\Phi = (a, b, c)^{\mathrm{T}} = (35, 8, 28)^{\mathrm{T}}$$

and the value of initial conditions of unknown parameters of the response system

$$\Phi_1(0) = (a_1(0), b_1(0), c_1(0))^{\mathrm{T}} = (10, 10, 10)^{\mathrm{T}}.$$

Case 1 Choose $J = \mathrm{diag}\{1, -1, -2\}$ and $N = 8$, to accomplish modified generalized projective synchronization in the coupled new 3D chaotic system with unknown parameters. Numerical simulation results are shown in Figs. 11(a)–11(f).

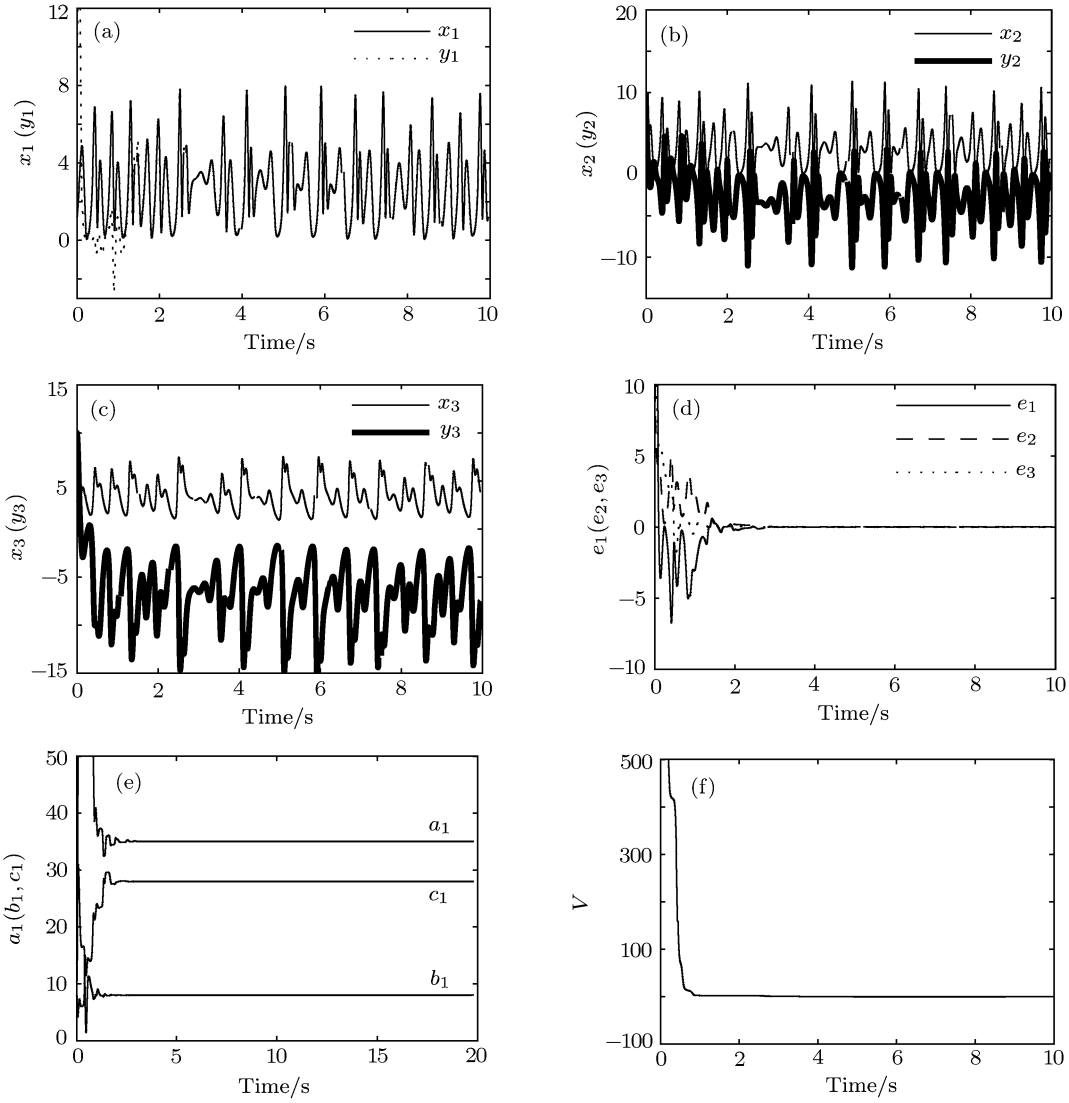
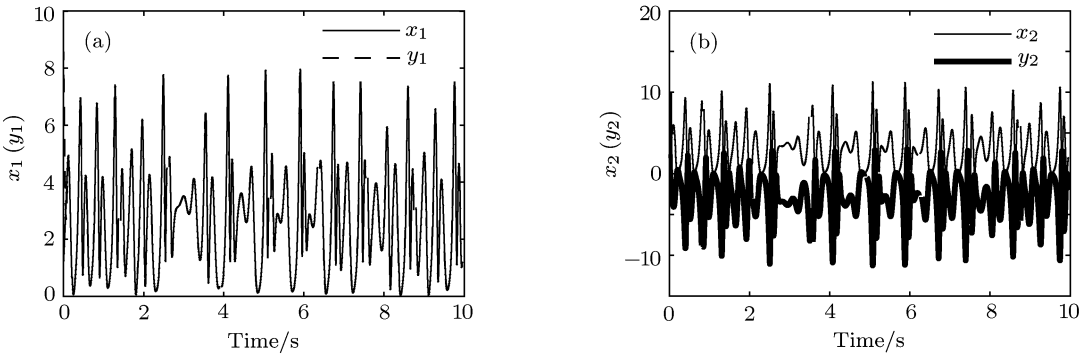


Fig. 11. (a) Time waveforms of state trajectories x_1 and y_1; (b) time waveforms of state trajectories x_2 and y_2; (c) time waveforms of state trajectories x_3 and y_3; (d) time waveforms of synchronization errors e; (e) time waveforms of unknown parameters Φ_1; (f) time waveforms of Lyapunov function.

Case 2 Choose $J = \mathrm{diag}\{1, -1, -2\}$ and $N = 30$, to accomplish modified generalized projective synchronization in the coupled new 3D chaotic system with unknown parameters. Numerical simulation results are shown in Figs. 12(a)–12(f).



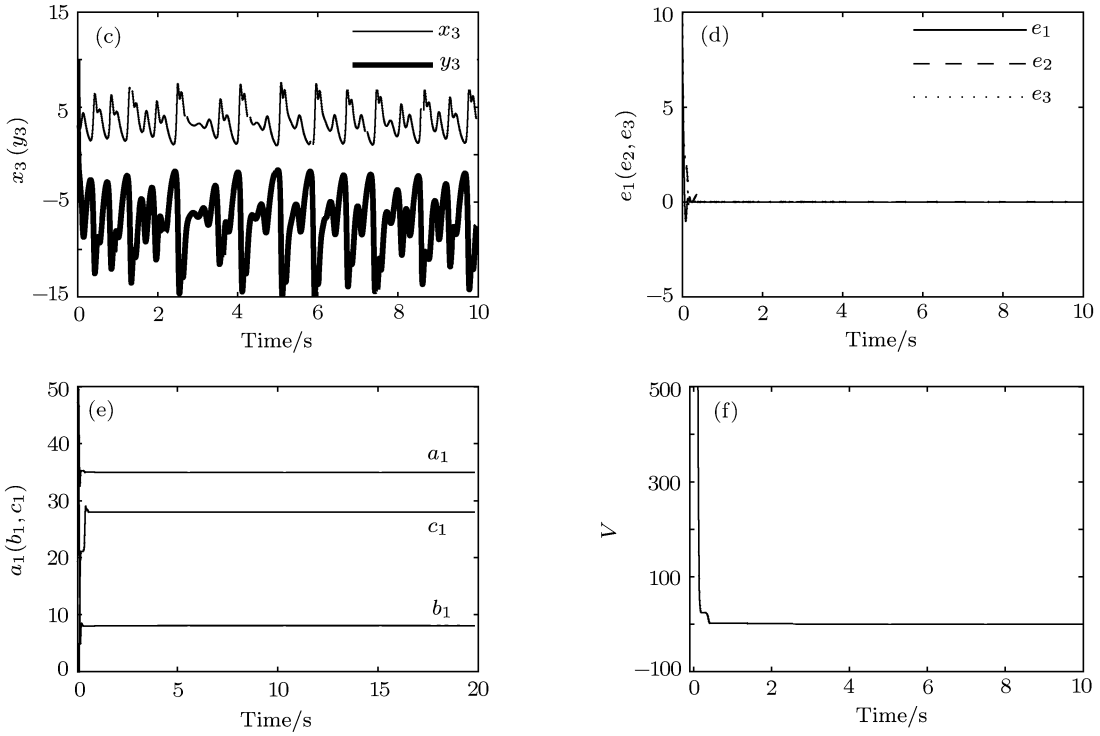


Fig. 12. (a) Time waveforms of state trajectories x_1 and y_1; (b) time waveforms of state trajectories x_2 and y_2; (c) time waveforms of state trajectories x_3 and y_3; (d) time waveforms of synchronization errors e; (e) time waveforms of unknown parameters Φ_1; (f) time waveforms of Lyapunov function.

From the above numerical simulation results, the limit of the error vector $e(t) = (e_1, e_2, e_3)^{\mathrm{T}}$ asymptotically approaches zero. So, through the drive-response method, we accomplish the modified generalized projective synchronization in the coupled new 3D chaotic system with unknown parameters and the unknown parameters $\Phi_1 = (a_1, b_1, c_1)^{\mathrm{T}}$ asymptotically approaching $\Phi = (a, b, c)^{\mathrm{T}}$. By increasing the control parameter N, we make the synchronization errors converge faster and synchronization effects be better. The unknown parameters $\Phi_1 = (a_1, b_1, c_1)^{\mathrm{T}}$ converge faster to $\Phi = (a, b, c)^{\mathrm{T}}$ and Lyapunov function also converges faster.

6. Conclusion

First, based on the Chen system and other chaotic system and by changing nonlinear terms and parameters of the Chen system, a new 3D chaotic system is constructed. Through researching into the basic dynamic behaviours of the new 3D chaotic system, we found that the new 3D chaotic system has abundant dynamic behaviours and has 4 real equilibrium points and 6 pairs of complex conjugate equilibrium points. Second, Lyapunov stability theory has been used and the control laws $u(t)$ and adaptive laws of parameters are designed to accomplish the modified generalized projective synchronization in the coupled 3D chaotic system with unknown parameters. Third, by improving the controller $u(t)$ and the adaptive laws of parameters in Ref. [13] and selecting the appropriate Lyapunov function, we find that the synchronization errors converge faster and the effect of synchronization is better in comparison with the method in Ref. [13].

References

[1] Lorenz E N 1963 *J. Atmos. Sci.* **20** 131
[2] Liu C X and Liu L 2009 *Chin. Phys.* B **18** 2188
[3] Zhang R X and Yang S P 2009 *Chin. Phys.* B **18** 3295
[4] Liu S, Liu B and Shi P M 2009 *Acta Phys. Sin.* **58** 4383 (in Chinese)
[5] Lü J H and Chen G R 2002 *Int. J. Bifurc. Chaos* **12** 659
[6] Liu C X, Liu T, Liu L and Liu K 2004 *Chaos, Solitons and Fractals* **22** 1031
[7] Pecora L M and Carroll T L 1990 *Phys. Rev. Lett.* **64** 821
[8] Chen M and Han Z 2003 *Chaos, Solitons and Fractals* **17** 709
[9] Li W L and Song Y Z 2008 *Phys. Rev. Lett.* **57** 51
[10] Hu J B, Han Y and Zhao L D 2009 *Acta Phys. Sin.* **58** 1441 (in Chinese)
[11] Zhang R X, Yang Y and Yang S P 2009 *Acta Phys. Sin.* **58** 6039 (in Chinese)
[12] Kuntanapreeda S 2009 *Phys. Lett.* A **373** 2837
[13] Liu F C and Song J Q 2008 *Journal of Dynamics and Control* **6** 130